E. W. Pugh

E. L. Boyd

J. F. Freedman

Angle-of-Incidence Anisotropy in Evaporated Nickel-Iron Films

Abstract: The magnetic anisotropies of iron, nickel, and permalloy films, evaporated onto glass substrates at various incident angles and substrate temperatures, have been measured by a torque method. For all compositions, the largest absolute value for the magnetic anisotropy occurs at the largest incident angle and lowest substrate temperature. A detailed calculation of the anisotropy resulting from a [111] fiber axis is found to fail to agree with the experimental results either in order of magnitude or in direction of the easy axis. The change in the magnetic anisotropies of films after removal from substrates is small enough that macroscopic stress cannot be the source of the anisotropy. A difference in electrical resistance parallel and perpendicular to a direction defined by the vapor stream during deposition is found to vary qualitatively very much like the magnetic anisotropy, both with film composition and incident angle. It is concluded that deposition at an angle of incidence produces an anisotropy in structural imperfections, which are interpreted in terms of shape and surface magnetic anisotropies as well as magnetostrictive effects.

Introduction

In films for possible device application, one of the most important parameters to be controlled is the magnetic anisotropy, since it affects the coercive force, the switching rate, and disturb sensitivity of the film. Such control has been achieved in the past only to a moderate degree by applying a suitable magnetic field during deposition, by maintaining the correct homogeneous composition throughout the film, and by careful control of the surface of the substrate and its temperature during deposition. More recently, however, it has been observed that the direction of the easy axis in permalloy films and the magnitude of the anisotropy is even more strongly affected by the angle of incidence of the vapor stream during deposition.[1] Various possible origins of this effect have been suggested: (1) the formation of Fe-Fe pairs in a predominantly nickel matrix, (2) the production of thickness gradients, (3) the formation of a crystalline texture axis, (4) the creation of an anisotropic strain in the film, or (5) the formation of anisotropic structural imperfections during deposition.

The first of these possibilities has been eliminated by the observation of the effect in pure nickel and pure iron films, where pair formation is impossible, while the second has been eliminated by the smallness of the magnetic anisotropy which could be predicted theoretically from considerations of thickness gradients.[1] The fiber axis and stress models, however, appeared to have been given considerable support by some recent work in iron films by Finegan and Hoffman[2] and by Knorr and Hoffman.[3] These works report the measurement of an anisotropic stress in an iron film evaporated at an angle of incidence as well as the measurement of magnetic anisotropy in a number of iron films evaporated at a 15° incident angle on substrates held at 75°C. This magnetic anisotropy is shown to be the same magnitude as would be predicted by the measured anisotropic stress combined with a [111] crystalline fiber axis tilted 10° from the normal to the film, as had been reported in the literature by Evans and Wilman.[4] Since the publication of these results, a number of studies of crystalline struc-

ture in evaporated films by x-ray and electron diffraction techniques have been reported.[5-8] While there is considerable lack of agreement among these papers, the evidence seems to suggest that in iron, nickel, or permalloy films, a [111] fiber axis may form normal to the film surface or with a slight inclination toward the vapor source of as much as 10°. The formation of [112] and [113] fiber axes has also been reported. All fiber axes tend to form at temperatures above 200°C more readily than at lower temperatures, and even the better fiber axis structures involve less than 50% of the total material. The above summary is in good agreement with our unpublished results using electron diffraction and x-ray diffraction techniques.[9]

The varying amounts and types of texture axes reported in films possessing similar magnetic anisotropies raise considerable doubt as to the validity of relating magnetic anisotropy to texture axis formation. Moreover, the theoretical basis for the model has been discredited for iron films by the work of Pugh et al,[10] in which it was demonstrated that a fiber axis structure yields too small a value for the magnitude of the anisotropy and also yields an anisotropy with the wrong sign. These results combined with the experimental observation that stress relief has little effect on the magnetic anisotropy, led the authors to discard the fiber axis and stress models for iron films and to propose that the magnetic properties result from the formation of anisotropic structural imperfections in the film during deposition at an angle of incidence. Similar models relating to structural imperfections have been proposed independently by Heidenreich and Reynolds[6] and by Smith et al.[8,11]

In the present paper, the previously reported work of the authors[10] on the angle-of-incidence effect in iron films is extended to include films of iron, nickel, and permalloy. As in the case of iron films, the magnetic anisotropy of nickel and permalloy films is shown to be incompatible with the fiber axis or stress models. Magnetic and electrical resistivity data are shown to be in qualitative agreement with the suggestion made in the previous paper, namely that the angle-of-incidence effects originate in anisotropically oriented imperfections; and an attempt is made to deduce the nature of the faults from considerations of shape and surface anisotropy.

Sample preparation

All samples were prepared in a vacuum system which utilizes an oil diffusion pump, a Meissner cold-trap, and a titanium getter to achieve a vacuum during deposition of about 10^{-6} mm Hg.[12] A few samples were deposited on freshly cleaved single crystals of NaCl so that they could be removed easily from the substrates. The remaining samples were deposited on glass disks 1 mm thick. To assure maximum reproducibility, all glass disks were cleaned ultrasonically in petroleum ether and then in succession were rinsed in distilled water, hydrofluoric acid, distilled water, and alcohol. All sample evaporations were made using the geometrical arrangement illustrated in Fig. 1. The tungsten filament was placed six inches from the first disk and at an angle of 20° from the normal. Angles of 27° and 34° from the normal were then achieved with the other two disks. Iron and nickel wire was wrapped around the center of the 4″ filament so that it covered about 2″ of the filament when melted for evaporation. The two rectangular slides parallel to the three samples were used for photometric chemical analysis and for optical thickness determinations. The thickness measurements are accurate to ±50 A, while an error of ±2% is anticipated on the chemical analysis.

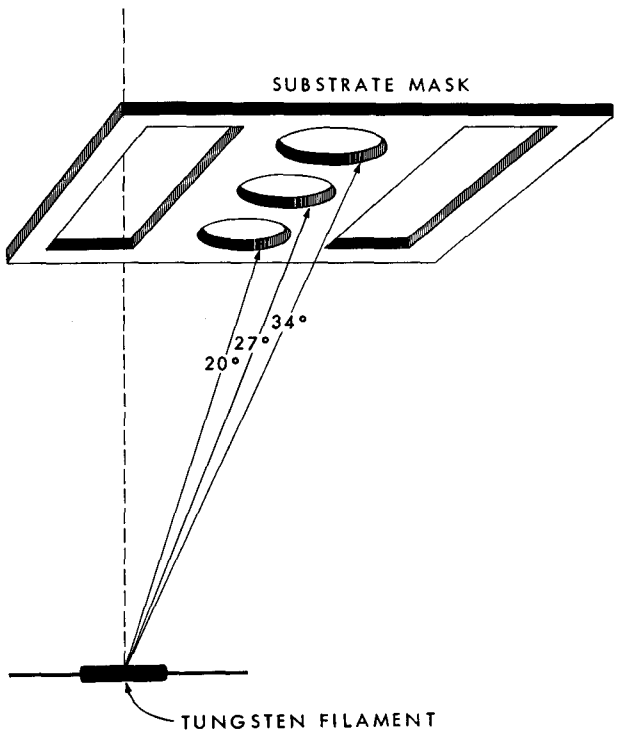

Figure 1 **Schematic drawing of evaporation geometry.**
The tungsten filament has about 1½″ of twisted nickel and iron wires wrapped about the center. Metal vapor streams upward through the mask onto glass slides at the indicated angles with the normals to the three round glass disks.

Before each evaporation the substrates were heated to 50°C above the deposition temperature and outgassed in the vacuum for ½ hour. The substrates were then cooled to the desired temperature and the metal deposited at about 60 A/sec. After deposition, the samples were cooled to room temperature in the vacuum and then removed for anisotropy determinations.

Anisotropy measurements

Because of the ambiguity which results from the determination of anisotropy by the standard hysteresis loop technique, especially when films have open loops in the hard direction, a torque balance was used for all meas-

urements recorded here. This balance has a sensitivity of 10^{-3} dyne-cm, which permits the detection of an anisotropy of $K_u=100$ erg/cc in a typical film containing 10^{-5} cc of material. Except for a few films in which K_u is less than 2×10^3 erg/cc, the major source of error is due to thickness determinations which yield errors of about $\pm5\%$.

The experimental data for iron, nickel, and permalloy films deposited at various temperatures onto glass are plotted in Fig. 2. It is evident that the larger magnitudes of anisotropy occur at low deposition temperatures and large incident angles. The anisotropy of iron films is also seen to be about an order of magnitude larger than that of permalloy or nickel films and of the opposite sign from nickel. Because of the geometry selected for evaporation, the films deposited at 34° are about 25% thinner than those deposited at 20°. Our previously reported results in iron films indicate that this thickness variation should have no effect on the magnetic anisotropies. In that work, each film was produced in a separate evaporation so that the film thickness was controlled independently of the incident angle. For those films, ranging in thickness from 400 to 2500 A, the variation of K_u with incident flux angle and substrate temperature was in good agreement with the present results and gives no indication of a thickness dependence.

Figure 2 **Uniaxial anisotropy constant K_u as measured in films deposited at various substrate temperatures.**
A possible anisotropy indicates that the easy axis is perpendicular to the vapor stream during deposition.

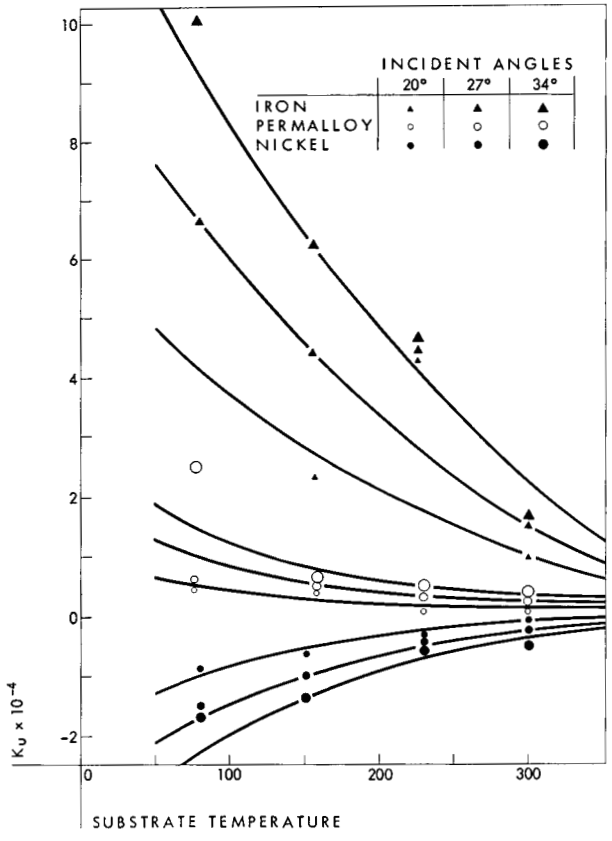

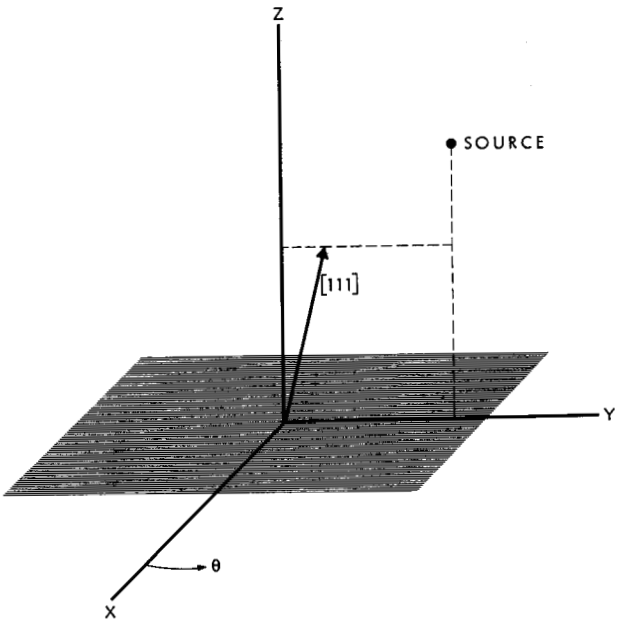

Figure 3 **A thin film in the xy plane deposited from a filament located in the yz plane.**
The resultant [111] fiber axis is inclined slightly from the z axis toward the filament.

Fiber axis model

Of the several models advanced to explain the angle-of-incidence effect, the fiber axis model has received the most attention recently. As applied to iron and nickel, this fiber axis structure can be represented by fixing a [111] direction of the bcc or fcc structure and allowing arbitrary rotation around this fixed direction. If the fixed [111] direction is chosen normal to the film surface, then isotropy results in the plane of the film. However, an anisotropy in the crystal structure and the magnetic properties in the plane of the film results when the fixed [111] direction is tilted from the normal toward the vapor source, as illustrated in Fig. 3. The resulting magnetic anisotropy may be calculated by making suitable coordinate transformations beginning with the phenomenological expression for the magnetic anisotropy energy in a cubic crystal:

$$E=K_1(\alpha_1^2\alpha_2^2+\alpha_2^2\alpha_3^2+\alpha_3^2\alpha_1^2)+K_2(\alpha_1^2\alpha_2^2\alpha_3^2)$$
$$+B_1(\alpha_1^2 l_{xx}+\alpha_2^2 l_{yy}+\alpha_3^2 l_{zz})$$
$$+B_2(\alpha_1\alpha_2 l_{xy}+\alpha_2\alpha_3 l_{yz}+\alpha_3\alpha_1 l_{zx}).$$

In this expression K_1 and K_2 are the crystalline anisotropy constants and the magnetoelastic coupling constants are given by $B_1=-(3/2)\lambda_{100}(C_{11}-C_{12})$ and $B_2=-3\lambda_{111}C_{44}$, where λ_{100} and λ_{111} are the magnetostrictive constants and C_{11}, C_{12}, and C_{44} are the elastic

constants. The α_i's are the direction cosines of the saturation magnetization relative to the crystallographic [100] axes, and the l_{ij}'s are the strain components relative to the same axes.

By neglecting the effects of stress, the following analytical expression for the magnetic anisotropy in the plane of the film can be obtained:

$$E=-(1/18)(9K_1-K_2)\sin^2\gamma\sin^2\theta + (1/12)(8K_1-3K_2)\sin^4\gamma\sin^4\theta + (2/9)K_2\sin^6\gamma\sin^6\theta,$$

where θ is measured in the plane of the film from the positive x axis. For fiber axis tilts of γ less than 16°, the $\sin^4\theta$ and $\sin^6\theta$ terms are less than 1/10 of the $\sin^2\theta$ term and may therefore be neglected, since a γ greater than 10° has never been obtained experimentally. Because it has not been possible to obtain an analytical expression for the anisotropy energy including the stress terms, the calculation has been performed numerically as a function of stress and fiber axis tilt using the method described by Knorr and Hoffman.[3] For tilt angles less than 16°, the anisotropy energy is found to be well expressed by the equations

$$E=K_u\sin^2\theta$$

and

$$K_u=-AS_x+BS_y-C,$$

where S_x and S_y are the stress components in the plane of the film, and the constants A, B, and C are functions only of γ. This calculation was programmed for both iron and nickel using the constants in Table 1, and the resulting graphs for A, B, and C as a function of fiber axis tilt are shown in Figs. 4 and 5, respectively.

Considering the case of iron, it is shown in Fig. 4 that if $S_x=S_y=0$, then K_u is negative and the y axis is the easy axis. The positive values for A and B are equivalent to negative magnetostrictive constants, and an anisotropic magnetostriction in the film results from the relative change in A and B as γ is increased. This deviation of B from A with increasing γ is due to the opposite signs of the magnetostrictive constants along the [100] and the [111] directions.

Comparing the calculated K_u with the experimentally determined values it is immediately evident that, for $S_x=S_y=0$ and the largest tilt angle reported ($\gamma=10°$), a theoretical value of $K_u=-7\times10^3$ is obtained. This value is an order of magnitude less than most measured values, even though the calculation assumes 100% fiber axis orientation, while diffraction work generally indicates less than 10% of the film to be so oriented. Even more important, theory predicts the y axis to be easy while experiment in all cases gives the x axis. Furthermore, since A is greater than B, any positive isotropic stress would make K_u even more negative. A negative

Figure 4 **Computed values of A, B, and C as functions of fiber axis tilt in an iron film.**

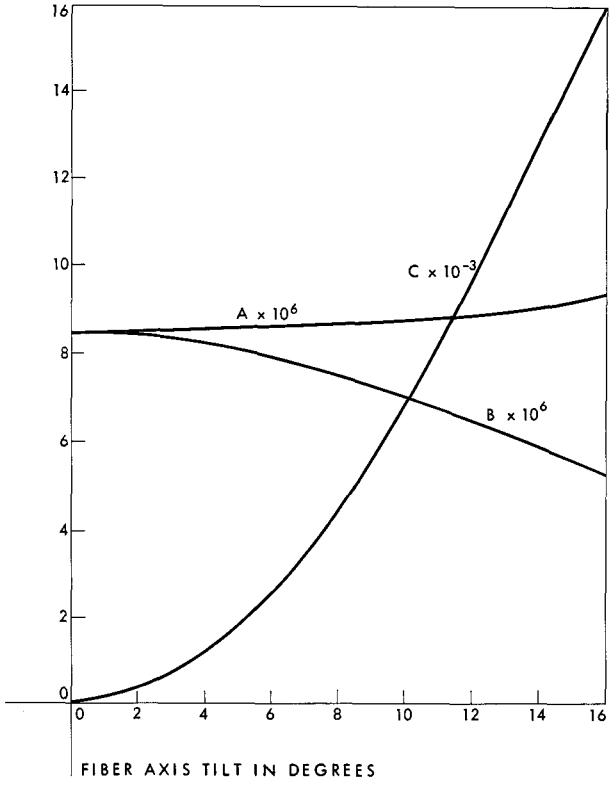

Figure 5 **Computed values of A, B, and C as functions of fiber axis tilt in a nickel film.**

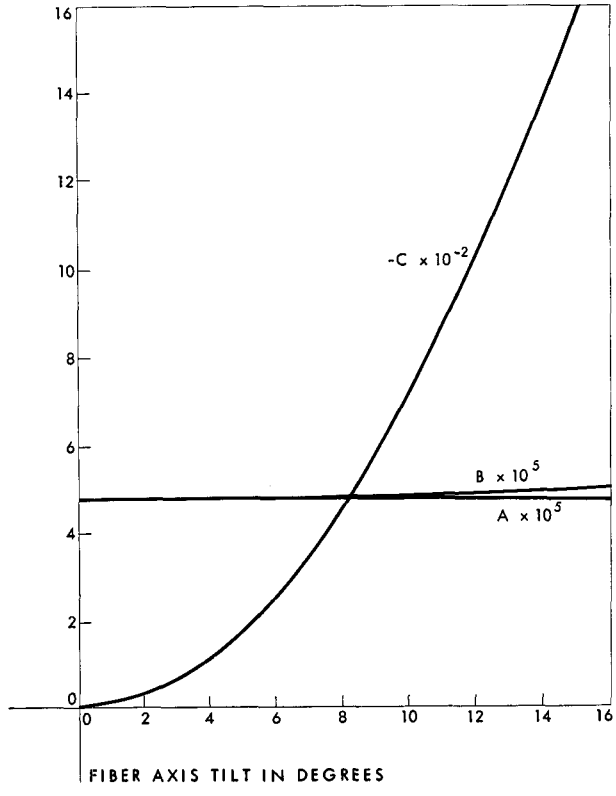

Table 1 **Constants used in fiber axis calculations.***

	K_1	K_2	λ_{100}	λ_{111}	C_{11}	C_{12}	C_{44}
Nickel	-4.5×10^4	2.3×10^4	-58×10^{-6}	-24×10^{-6}	2.5×10^{12}	1.6×10^{12}	1.18×10^{12}
Iron	45×10^4	7.1×10^4	20×10^{-6}	-16×10^{-6}	2.29×10^{12}	1.34×10^{12}	1.14×10^{12}

* K_1 and K_2 were taken from H. Sato and B. S. Chandrasekhar, *The Phys. and Chem. of Solids* **1,** 228 (1957).
Values for λ_{100} and λ_{111} were taken from R. C. Hall, *J. Appl. Phys.* **30,** 816 (1959).
Values for C_{11}, C_{12}, and C_{44} for iron were taken from W. B. Daniels, M. S. thesis, Case Inst. of Tech., unpublished, 1955.
Values for C_{11}, C_{12}, and C_{44} for nickel were taken from E. W. Lee, *Rep. on Prog. in Phys.* **XVIII,** 184 (1955).

Table 2 **Magnetic anisotropy of films deposited on NaCl.**

Sample		% Ni	% Fe	*Thickness, angstroms*	*Deposition temperature,* °C	$K_u\times10^{-4}$ *before removal*	$K_u\times10^{-4}$ *after removal*
315	20	100		990	75	−1.4	−1.4
	27	100		670	75	−4.0	−8.0
	34	100		530	75	−3.9	−1.4
346	20	100		1500	105	−2.98	−3.39
	27	100		1340	105	−3.56	−3.20
	34	100		1120	105	−4.25	−6.32
316	20	78	22	1100	75	0.86	1.13
	27	78	22	930	75	1.12	1.84
	34	78	22	815	75	2.7	−1.18
322	20		100	795	85	2.64	3.24
	27		100	650	85	6.15	4.98
	34		100	600	85	7.30	8.90
319	20		100	1300	150	0.58	0.55
	34		100	1000	150	4.08	5.52

isotropic stress could make K_u less negative; however, the stress in films evaporated onto glass is always observed to be positive. Only a stress which is much larger in the y than the x direction could account for the positive K_u in a manner consistent with the fiber axis model. This possibility is not considered until the next section, because the effect of anisotropic stress in an unoriented iron film differs very little from that in a film with 100% fiber axis structure, owing to the similarity in magnetostriction constants for the two cases: $\lambda\cong-7\times10^{-6}$ in the former case and $\lambda_{eff}\cong-5.7\times10^{-6}$ in the latter.

Using the same line of reasoning for the nickel films, it is readily seen from Fig. 5 that theory predicts an anisotropy an order of magnitude too low, the wrong direction for the easy axis, and no detectable anisotropy with isotropic stress. The inadequacies of the model are even more evident in the case of permalloy, for which the magnetocrystalline anisotropy constants and the magnetoelastic energy all approach zero. For all three materials, K_u decreases with increasing substrate temperature during deposition even though the better fiber axis structures are observed at the higher deposition temperatures. Thus for films deposited at temperatures up to 300°C, the fiber axis structure has been shown to have a negligible effect on the uniaxial magnetic anisotropy.

Anisotropic stress model

In order to investigate the possibility that a macroscopic anisotropic stress could be responsible for the observed anisotropy of films evaporated at an angle of incidence, a series of films were deposited on rock salt at a temperature below which significant epitaxy takes place; and the magnetic anisotropy was measured for each film before and after removal from the substrate. After removal, any macroscopic strains created in the film during deposition would be relieved. Removal was accomplished by lowering the substrate slowly into water so that enough NaCl was dissolved to leave the film floating on the water. It was then picked up on a glass slide and the water evaporated from the film. The values of K_u as measured before and after removal from the substrate are listed in Table 2. It is evident that anisotropies of

films deposited on NaCl substrates are essentially the same as for films made on glass, although perhaps a little higher, especially in the case of nickel films. Furthermore, with the exception of one film (316-34), all films retained the same easy axis and the same magnitude of the anisotropy within a factor of two, thus indicating that macroscopic stress is not the major source of magnetic anisotropy. A similar result has recently been reported by Heidenreich and Reynolds,[6] who evaporated permalloy films at an angle of incidence onto carbon-coated glass slides and observed little change in anisotropy after stripping the films from the substrates.

Evidence for structural imperfections

As a result of the preceding experiments and theoretical considerations, all previously suggested causes of the angle-of-incidence induced anisotropy have been eliminated with the exception of the proposed anisotropic alignment of structural imperfections. This suggestion is well supported by the decrease in K_u with increasing substrate temperature, since at elevated temperatures the atomic migration on the substrate would be enhanced and the probability of forming imperfections decreased. The suggestion is further supported by the small and almost random changes observed in the magnitude of the anisotropy when films were floated off rock salt. It was in fact noted that the change was greatest when the process was accompanied by severe cold working and was generally less than 20% when it was possible to remove the films without bending them more than about 30°. An obvious experiment to test the randomness of the effect is to compare the changes observed in films floated off NaCl so that the bending is parallel to the easy axis with those bent perpendicular. A record of this was kept for all films, but no correlation was detected.

In order to learn more about the nature of the structural imperfections, the electrical resistivities of a number of films were measured both parallel and perpendicular to the source direction, and the resulting differences were compared with the magnetic anisotropies of the same films. It was anticipated that a gross anisotropy in structural defects could give rise to an anisotropy in resistance associated with the imperfection scattering of the conduction electrons. For this experiment, a series of films ranging in composition from pure nickel to pure iron were evaporated onto glass substrates which were cleaned in the usual manner. The evaporation geometry was as illustrated in Fig. 1, and the substrate temperature was held at 100°C for all films. The electrical measurements were made at room temperature by a dc four-probe method with a reproducibility of better than $\pm 0.3\%$.

To obtain absolute resistivities by this method for the circular films used in these experiments, a shape correction was made as determined by solving the boundary value problem for the current flow. Measurements were made on the film with no magnetic field applied and also with a field applied parallel to the current flow. The magnetoresistance effect measured was less than 1.5% for all compositions. This is much less than the values measured for bulk material but is in agreement with work by Rappeneau,[13] which indicates that the magnetoresistance of pure nickel films is less than that for bulk material and decreases with decreasing thickness of the film. The results indicate that the magnetoresistance contribution to the absolute resistivities of the films may be neglected; however, it would significantly affect the difference of the resistivities measured parallel and perpendicular to the vapor source direction, since this difference varies from as little as ½% to little more than 7% of the absolute value. Such a contribution to the resistivity anisotropy was eliminated in this work by saturating the films parallel to the direction of current flow by a field of about 400 oe for all measurements.

The resistivity parallel to the source direction minus that perpendicular divided by the perpendicular resistivity is defined as Δ. Values for the total resistivity and for Δ for all films are listed in Table 3 along with the uniaxial anisotropy K_u, as determined by the torque balance. The lower resistance for all films (with only one exception) was found to be perpendicular to the incident flux direction. As in the case of magnetic anisotropy, the larger resistive anisotropies occur at large incident angles and in the iron-rich films. However, unlike the values of K_u the Δ's do not change sign at 10% iron in nickel. This change in sign of K_u and failure of Δ to change sign is one of the more interesting aspects of the angle-of-incidence effect.

In Fig. 6 the total resistivities of the films as measured in the "easy" resistivity direction are compared with those of bulk samples determined by Shirakawa.[14] Except in the region from 50% to 80% iron, which is very likely a two-phase $(\alpha+\gamma)$ region, the films exhibit a resistivity considerably higher than that of bulk, but possessing the same general variations with composition. The difference between film and bulk resistivities is further seen to increase with increasing angle of incidence. It is tempting to associate all of the difference between bulk and film resistivities with structural imperfections created during deposition. However, a rather large portion may be due to surface scattering of the conduction electrons; and as was pointed out earlier, the thickness of films produced with a 34° angle of incidence tends to be about 25% less than that of those produced at 20°. The dependence between angle-of-incidence and thickness built into this experiment tends to mask the effect of angle-of-incidence on total resistivity, since thickness variations would produce a similar effect. Nevertheless, it is unlikely that all of the increased resistivity of these films is caused by surface scattering. Copper films 800 A thick exhibit a resistivity increase of less than 30% due to surface scattering, as compared to an increased resistivity of our nickel films over bulk values of 80%, in spite of the longer mean free path in copper. It might be estimated crudely that structural imperfections contribute a resistivity of 6 ± 3 microhm-cm over the range from pure nickel to 50% iron in

nickel for films deposited at an angle of 20°. (This is equivalent to a 20% to 70% increase in resistivity.) Thus, due to the relatively large contribution of imperfection scattering to the total resistivity, a given anisotropy in the total measured resistivity may well represent only a slightly larger anisotropy in the contribution from imperfections.

In Fig. 7, K_u and Δ have been plotted as functions of iron concentration for the 34° angle-of-incidence films. (While K_u and Δ are smaller for the 20° and 27° films, the variation with composition is essentially the same and supports the shape of the curve chosen to pass through the data points in Fig. 7.) The vertical bars through the resistivity points indicate the anticipated experimental error while for the magnetic anisotropy errors are little larger than the points themselves. Although the curves for K_u and Δ are not identical, there is a striking similarity.

Both the magnetic and resistivity anisotropies increase with increasing iron content, peak in the vicinity of 50% iron, diminish, and then peak again at 80% iron. The relatively gradual change of Δ with composition and its constancy of direction give no reason to suspect a major change in the structural form of the imperfections near the 10% iron composition. The change in sign of the magnetic anisotropy should therefore be explained in terms of magnetic interactions and not structural changes.

Table 3 **Resistive and magnetic anisotropies of Ni-Fe films.**

A) *Percent* Fe
B) *Angle in degrees*
C) *Thickness in angstroms*
D) $\rho_\perp$ *in microhm-cm*
E) $\Delta \times 10^2$
F) $K_u \times 10^{-4}$ *in erg/cc*

A	*B*	*C*	*D*	*E*	*F*	*A*	*B*	*C*	*D*	*E*	*F*
0.0	20	1080	15.87	0.5	−0.70	58.2	20	830	48.24	1.4	0.96
	27	875	15.70	0.5	−0.97		27	795	54.68	0.7	2.96
	34	750	17.08	0.5	−1.04		34	655	55.38	4.4	5.73
7.5	20	1130	19.15	0.0	−0.21	62.1	20	1310	38.68	−1.7	1.76
	27	995	20.49	1.0	−0.41		27	1260	44.48	1.5	3.20
	34	840	22.11	1.7	−0.55		34	925	42.18	3.9	9.99
12.5	20	1045	22.33	0.7	0.16	68.8	20	1320	32.13	1.1	1.78
	27	990	26.18	1.1	0.17		27	1150	34.33	2.8	4.40
	34	730	25.42	2.5	0.73		34	970	36.90	5.8	7.28
20.0	20	875	22.50	0.8	0.40	58.6	20	880	49.60	0.3	0.91
	27	775	25.45	1.1	0.56		27	840	55.02	1.5	1.88
	34	710	30.61	3.1	1.12		34	780	64.70	3.8	4.90
29.3	20	575	28.88	2.2	0.79	67.9	20	1040	29.72	0.9	3.61
	27	520	32.83	2.1	1.07		27	985	32.75	1.6	5.50
	34	510	42.55	2.6	1.10		34	895	38.67	4.7	6.44
29.6	20	890	26.99	1.7	0.86	78.0	20	1470	37.00	2.5	7.80
	27	815	30.70	3.0	0.64		27	1150	34.80	3.8	17.39
	34	695	33.88	4.1	1.21		34	1030	39.75	6.7	19.42
30.8	20	1025	26.76	0.4	1.37	85.2	20	1240	38.72	1.4	4.72
	27	920	29.69	1.6	0.79		27	1150	43.10	3.6	9.45
	34	675	28.28	4.4	2.28		34	720	33.59	5.0	21.79
40.0	20	655	38.56	3.5	1.99	85.6	20	1345	37.35	2.0	8.21
	27	605	—	—	2.56		27	1200	39.64	3.2	15.23
	34	530	53.25	6.0	5.04		34	1080	44.01	6.5	19.67
44.3	20	995	43.55	0.7	1.80	100	20	1340	18.54	1.7	0.78
	27	850	46.71	2.1	2.93		27	1145	18.49	2.7	4.86
	34	700	50.46	7.1	6.92		34	1010	20.37	5.3	9.14
53.3	20	980	43.39	3.0	3.10	100	20	1590	20.71	1.3	1.39
	27	795	42.07	1.6	6.03		27	1390	22.70	2.4	5.39
	34	680	46.41	4.0	9.44		34	1095	22.68	7.5	9.19

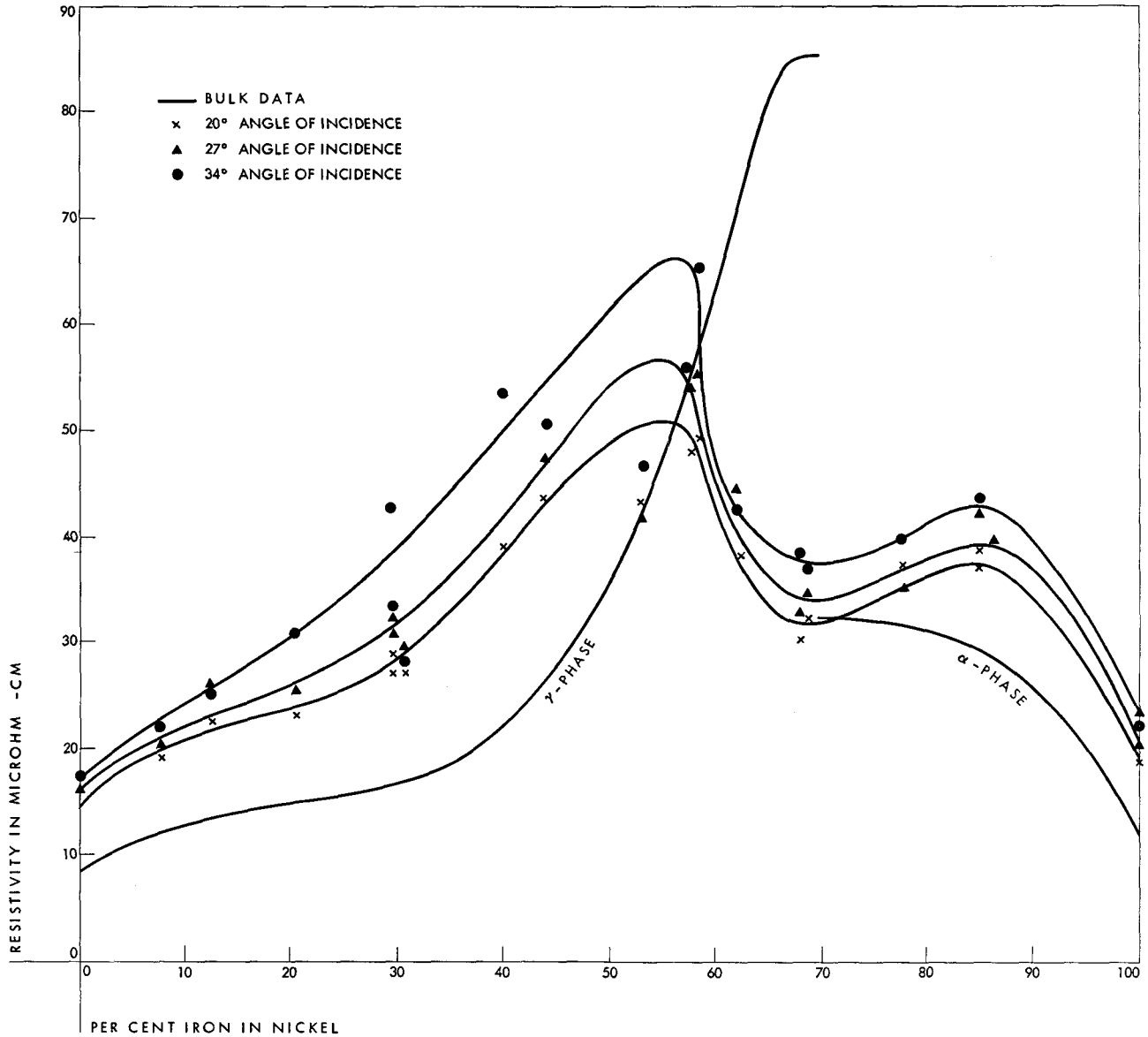

Figure 6 **Resistivities of bulk Ni-Fe alloys and Ni-Fe films given at various angles of incidence plotted as a function of composition.**

Structural imperfection models

Because of the apparent importance of (111) stacking faults and oxygen content to magnetic annealing in permalloy as recently reported,[15] it seems justified to relate the structural imperfections in films to these faults. The effect of these faults on electrical conductivity would be significantly increased if they held quantities of oxygen impurities. Magnetic anisotropies could then be related to iron-oxygen or nickel-oxygen interactions. While a detailed theoretical understanding of this phenomenon is not in sight, it is interesting that neutron diffraction studies of antiferromagnetic NiO and FeO structures indicate that the spins lie parallel to the (111) plane in NiO and perpendicular to it in FeO.[16] This could give a qualitative explanation for the change in sign of K_u which occurs at 10% iron content; however, it is difficult to resolve this model, for a room-temperature effect, with the measured Néel temperature of FeO well below room temperature. It is, of course, possible that Fe_3O_4 with preferred orientation is formed in the material. However, to account for $K_u=6\times10^4$ erg/cc as observed in a pure iron film, far more than 20% of the film would have to be oriented Fe_3O_4, and this is inconceivable. Moreover, the work of Nesbitt et al[15] indicates that the annealed easy direction in permalloy is

perpendicular to (111) stacking faults, while the present conductivity data suggest that the iron-rich alloys have their easy direction parallel to the larger dimension of the inclusion, since one would anticipate the lower resistivity direction to be *parallel* to the faulted planes.

Another approach is to postulate an anisotropic distribution of grain boundaries or faults with their planes parallel to the low resistance. A simple analytical approach is then to treat these sheets of imperfections as nonmagnetic inclusions—a procedure which may be justified by the altered crystalline bonding along the fault or by the presence of nonmagnetic impurities, e.g., oxides, along the imperfection sheet. Qualitatively the analysis of the magnetic effect of the faults is then the same as for anisotropic vacancy clusters; in either case, an explanation cannot be achieved with shape anisotropy alone because of the change in sign of K_u as the composition passes through 10% Fe. However, it has been pointed out by Néel[17] that the magnetic interactions experienced by spins lying on a surface (e.g., the surface of a void or nonmagnetic inclusion) are quite different from those of spins lying within the bulk of the material. A pseudo-dipolar coupling approximation for the surface anisotropy of these nonmagnetic inclusions reveals that spins have their lowest energy in nickel when perpendicular to a (111) surface.

Assuming a surface anisotropy constant of approximately 1 erg/cm^2 for nickel, the total area of nonmagnetic inclusions parallel to the low-resistivity direction minus that perpendicular required to produce the observed K_u of 10^4 erg/cc is approximately 10^4 cm^2/cc of material. For inclusion sheets one atom wide, approximately two parts per thousand of the total material would be nonmagnetic. If one postulates no change in surface area of the inclusions in going to a composition of 10% iron, then a pseudo-dipolar coupling calculation for surface anisotropy would indicate a decrease in K_u of only a factor of two. The correct amount of shape anisotropy needed to force K_u to zero at this composition is therefore of the order of 10^4 erg/cc. Attributing a demagnetizing factor of 4π to the inclusions, the postulated nonmagnetic sheets need to be about 20 lattice spaces wide and would occupy about ½% of the total volume if they were perfectly oriented. It should be emphasized, however, that this argument is applicable only if the surface of the nonmagnetic inclusion lies in a

Figure 7 **Magnetic and resistivity anisotropies plotted as a function of film composition for films deposited at an angle of incidence of 34° and substrate temperature of 100°C.**

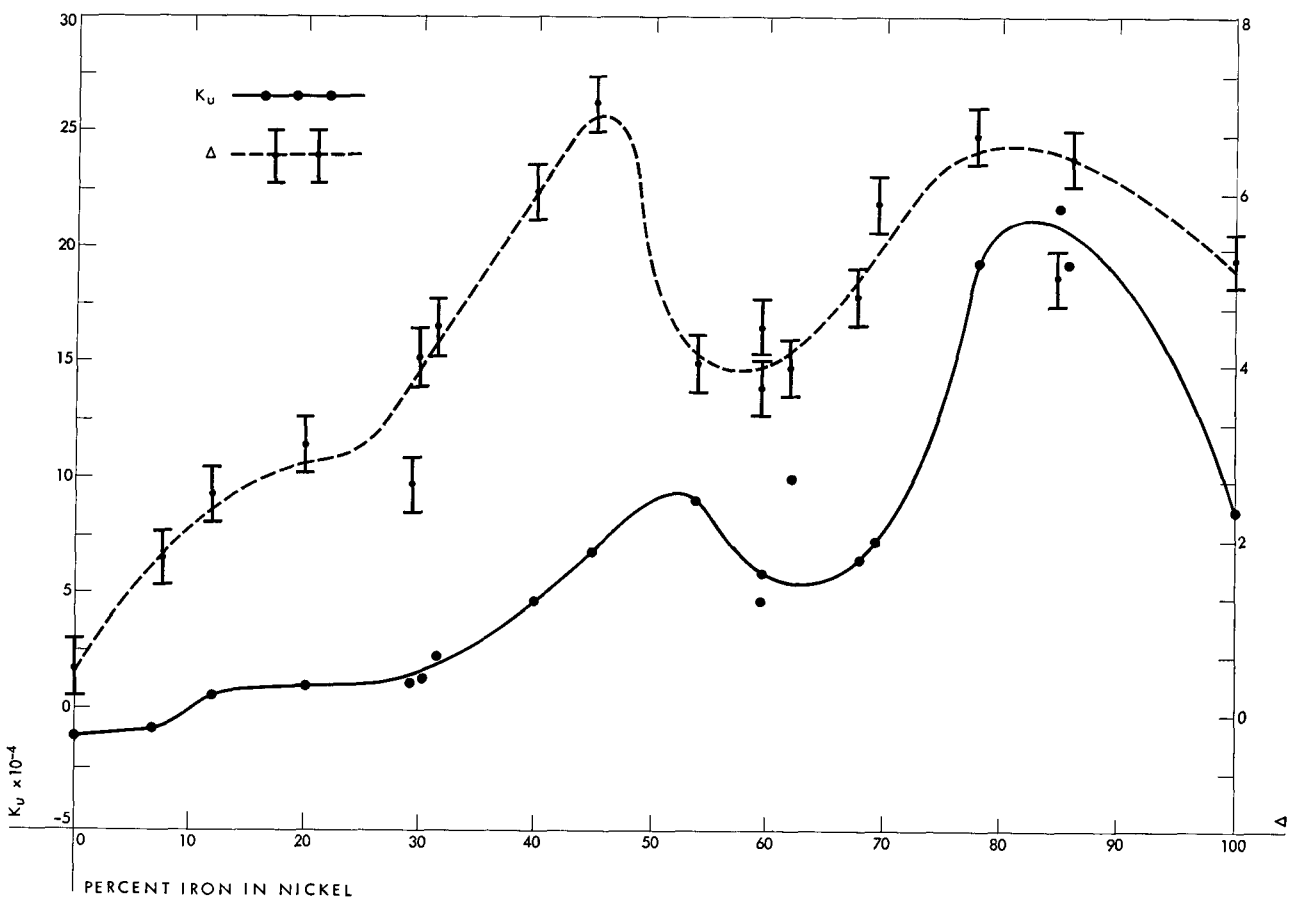

(111) plane relative to the nickel-rich alloy. If the inclusions occur along the randomly oriented crystallographic plane, Néel's calculation indicates the easy axis would be parallel, rather than perpendicular, to the long dimension of the inclusions in nickel.

Perhaps the simplest model of all is to assume that the major magnetic effect associated with the inclusions is a shape anisotropy. This accounts for the sign of the anisotropy from 10% iron to pure iron, and the change in sign near nickel may be attributed to the large negative magnetostrictive constant of nickel-rich alloys if a compressional force normal to the surface of the inclusion is postulated.[18] Assuming a relatively constant structural imperfection from pure nickel to pure iron, the value of K_u would be proportional to the magnetization squared plus some constant times the magnetostrictive constant. The former rises continuously from nickel to iron with the exception of a sharp minimum near 70% iron, while the latter goes from a large negative value for nickel to a large positive value at 50% iron followed by a minimum at 70% iron, a maximum at 80% iron, and then a sharp drop to a slightly negative value for pure iron. The variation of K_u predicted qualitatively by this model over the entire range of composition is excellent and requires about one percent of the material to be nonmagnetic inclusions. However, the model does not explain the similar compositional dependence of Δ, unless it is assumed (and not unreasonably so) that the sharp changes in the spin direction of atoms lying near the imperfections contribute significantly to the scattering of the conduction electrons.

While the evidence presented here points conclusively toward structural imperfections, none of the models describing these imperfections has been fully satisfactory. To obtain a satisfactory understanding of the angle-of-incidence effect, considerably more experimental work is needed. In particular, the effect of oxygen must be examined by fabrication of films in vacuums of 10^{-8} mm Hg or better, important preparation parameters such as rate of deposition must be studied, and finally, more evidence is needed from electron microscopy and diffraction studies.

Acknowledgments

The authors are indebted to Drs. S. Chikazumi and L. R. Bickford for helpful discussions during the preparation of the manuscript, to J. Matisoo and R. Matick for programming the fiber axis calculations, and to W. Kately for preparation of the thin film samples.

References and footnotes

1. D. O. Smith, *J. Appl. Phys.* **30,** 264S (1959).
2. J. D. Finegan and R. W. Hoffman, *J. Appl. Phys.* **30,** 597 (1959).
3. T. G. Knorr and R. W. Hoffman, *Phys. Rev.* **113,** 1039 (1959).
4. D. M. Evans and H. Wilman, *Acta Cryst.* **5,** 731 (1952).
5. R. R. Verderber, *J. Appl. Phys.* **30,** 1359 (1959).
6. R. D. Heidenreich and F. W. Reynolds, *Proceedings of the International Conference on Structure and Properties of Thin Films,* p. 402, John Wiley, 1959.
7. R. F. Adamsky, Magnetics Conference, Detroit, November (1959).
8. M. S. Cohen, E. E. Huber, G. P. Weiss, and D. O. Smith, Magnetics Conference, Detroit, November (1959).
9. The authors are indebted to D. P. Cameron and C. F. Aliotta of this laboratory for help with electron diffraction and to R. Giedd and E. C. de Wys of the IBM Kingston Laboratory for help with x-ray diffraction studies.

Received November 20, 1959

10. E. W. Pugh, J. Matisoo, D. Speliotis, and E. L. Boyd, Magnetics Conference, Detroit, November (1959).
E. W. Pugh, *Proceedings of the International Conference on Structure and Properties of Thin Films,* p. 408, John Wiley, 1959.
11. D. O. Smith, E. E. Huber, M. S. Cohen, and G. P. Weiss, Magnetics Conference, Detroit, November, 1959.
12. For a detailed discussion of this system see Conventional Evaporator B with Meissner trap in the article on vacuum systems by H. Caswell, this issue, p. 130.
13. T. Rappeneau, *Cahiers de Physique* **12,** 185 (1958).
14. Y. Shirakawa, *Sci. Repts. Tohoku Imp. Univ.* **27,** 485 (1939).
15. R. D. Heidenreich, E. A. Nesbitt, and R. D. Burbank, *J. Appl. Phys.* **30,** 995 (1959).
E. A. Nesbitt and R. D. Heidenreich, *J. Appl. Phys.* **30,** 1000 (1959).
E. A. Nesbitt, R. D. Heidenreich, and A. J. Williams, Magnetics Conference, Detroit, November, 1959.
16. W. L. Roth, *Phys. Rev.* **110,** 1333 (1958).
17. L. Néel, *Compt. Rend.* **237,** 1468 (1953).
L. Néel, *J. Phys. et Radium* **15,** 225 (1954).
18. The "needle structure" recently suggested by Smith et al (Ref. 11 above) to explain their observations in permalloy is qualitatively very similar to this model.